Pure and doped boron nitride nanotubes

More than ten years ago, it was suggested theoretically that boron nitride (BN) nanotubes could be produced. Soon after, various reports on their synthesis appeared and a new area of nanotube science was born. This review aims to cover the latest advances related to the synthesis of BN nanotubes. We show that these tubes can now be produced in larger amounts and, in particular, that the chemistry of BN tubes appears to be very important to the production of reinforced composites with insulating characteristics. From the theoretical standpoint, we also show that (BN)-C heteronanotubes could have important implications for nanoelectronics. We believe that BN nanotubes (pure and doped) could be used in the fabrication of novel devices in which pure carbon nanotubes do not perform very efficiently.

M. Terrones[1,2]*, J. M. Romo-Herrera[1], E. Cruz-Silva[1], F. López-Urías[1], E. Muñoz-Sandoval[1], J. J. Velázquez-Salazar[1], H. Terrones[1], Y. Bando[2,3], and D. Golberg[3]

[1]Advanced Materials Department, IPICYT, Camino a la Presa San José 2055, Col. Lomas 4 sección, San Luis Potosí, 78216, México
[2]International Center for Young Scientists (ICYS), National Institute for Materials Science, Namiki 1-1, Tsukuba, Ibaraki 305-0044, Japan
[3]Nanoscale Materials Center, National Institute for Materials Science, Namiki 1-1, Tsukuba, Ibaraki 305-0044, Japan
*E-mail: mterrones@ipicyt.edu.mx

Hexagonal boron nitride (h-BN) is a layered material analogous to graphite that exhibits a hexagonal crystal structure (lattice parameters: a = 2.50 Å, c = 6.66 Å; Fig. 1a). In this material, the hexagonal layers eclipse one another (aA, aA,... stacking) and the B_3N_3 hexagons overlap and alternate with N_3B_3 hexagons (Figs. 1a and 1b). From the electronic standpoint, h-BN is an insulator with a bandgap of ~5.8 eV (Fig. 1c)[1]. In addition, the in-plane thermal conductivity of h-BN experimentally oscillates between 200 W/mK and 500 W/mK.

However, the properties of bulk h-BN are expected to be different to finite BN nanoscale structures. In this context, the idea of rolling up individual hexagonal sheets of BN to form nanotubes (similar to carbon nanotubes) was first proposed in 1994 by Rubio *et al.*[2]. The authors demonstrate, using a simple tight-binding approach, that such BN nanotubes (BN NTs) would behave as semiconductors (Fig. 1d) with bandgaps typically larger than 2 eV (the larger the diameter of the tube, the larger the bandgap)[2]. It is worth mentioning that pure carbon nanotubes (CNTs) are able to behave as metals or
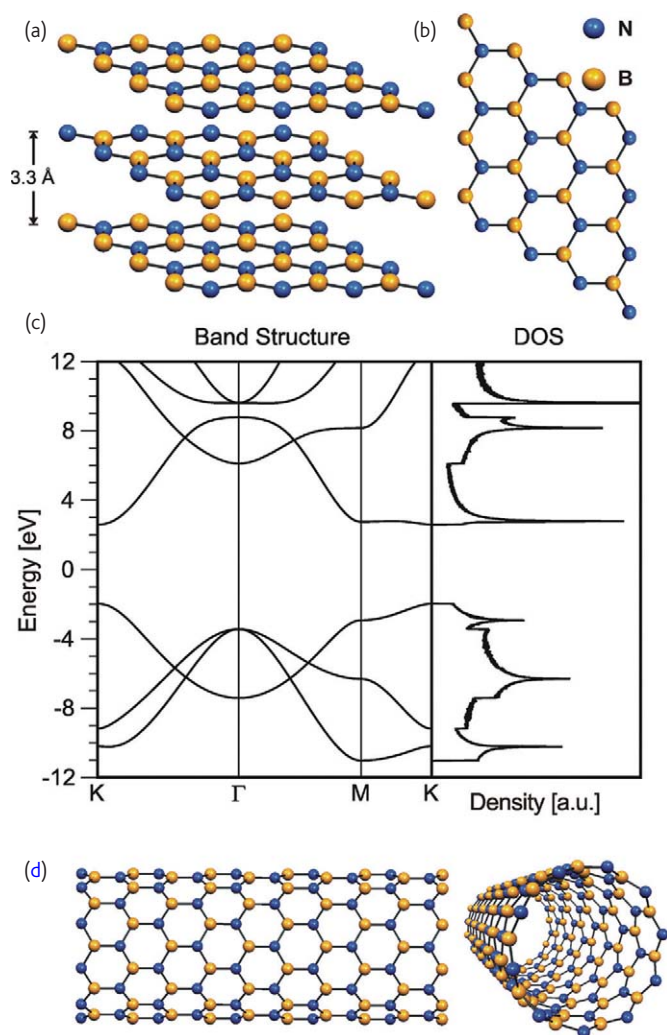
Fig. 1 (a) Molecular model depicting the structure of h-BN; note the three layers and the interlayer spacing of 0.33 nm; (b) top view of h-BN showing alternating B and N atoms; (c) calculated band structure and density of states for a single sheet of h-BN showing that this material is an insulator with a bandgap of ~4.5 eV (E_f located at zero). Note that this local density approximation calculation underestimates the band gap; other studies considering the GW approximation reveal a bandgap of 5.4 eV for bulk h-BN and 6.0 eV for a single h-BN layer; and (d) molecular model of a BN NT exhibiting a (10,0) zigzag chirality (two views are depicted).

semiconductors, depending on the chirality (the way the hexagonal rings are aligned with respect to the tube axis)[3,4]. Therefore, more sophisticated theoretical approaches have been used to determine the stability, feasibility, and electronic properties of BN NTs. To this end, Blase et al.[5] used the local density approximation (LDA) to determine that BN NTs are insulating with a bandgap of ~5.5 eV and that this gap is nearly independent of tube diameter, chirality, and number of tube walls. However, we should emphasize that it has been predicted that extremely narrow BN NTs (e.g. diameters of 2 Å) could exhibit semiconducting behavior with bandgaps close to 1 eV, whereas the
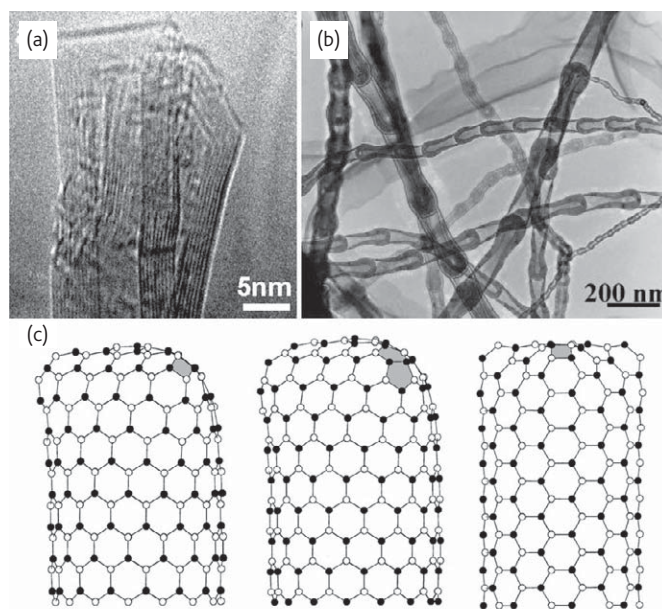
Fig. 2 (a) High resolution transmission electron microscopy (HRTEM) image of a multiwalled BN NT produced using the arc discharge method with Ta and BN electrodes; (b) TEM image of bamboo-like BN NTs synthesized from an amorphous B-N-O precursor with a low oxygen content of ~10 at% (courtesy of R. Z. Ma); and (c) molecular models of various possible closed single-walled BN NTs by adding squares and adjacent pentagons (pentalene) in different ways; note that squares and pentagons are indicated in gray. (Adapted from[9].)

electronic properties of larger diameter BN NTs (~4 Å; (10,0) or (5,5) chiralities) behave nearly as bulk h-BN. The former behavior can be explained in terms of the hybridization caused by the strain on narrow diameter tubes. Unfortunately, these highly strained BN NTs seem to be unstable under ambient conditions.

Synthesis
Arc discharge
Following theoretical predictions, scientists started to synthesize BN NTs and nanostructures experimentally. In 1995, Chopra et al.[6] reported the production of multiwalled BN NTs using arc-discharge techniques involving a tungsten electrode filled with h-BN powder (anode) and a copper electrode (cathode). These tubes always contain a metal particle at their tips and exhibit an interlayer separation of ~3.3 Å, which is consistent with the interplanar distance of bulk h-BN. Subsequently, a French group lead by Loiseau reported the production of BN NTs by arcing HfB_2 electrodes in an inert atmosphere[7]. This technique leads to the formation of single- and double-walled BN NTs. In this case, the NTs display closed square caps because of the presence of three B_2N_2 squares. Simultaneously, Terrones et al.[8] reported the formation of BN NTs by arcing Ta-BN electrodes under N_2. In this case, it was found that the nanotube caps exhibit both metal particles and/or square morphologies[9] (Figs. 2a and 2c). In 2000, Cumings and Zettl[10] reported the production of large quantities of double-walled BN NTs by arcing B electrodes containing 1 wt.% of Ni or Co in a N_2 atmosphere.

Laser ablation

The second synthesis method reported for the production of BN NTs is the laser assisted technique. In this technique, single-crystal cubic BN (c-BN) specimens are laser heated for 1 min in a diamond anvil cell under N_2 pressures of 5-15 GPa. High-resolution transmission electron microscopy (HRTEM) of samples produced in this way reveals multiwalled NTs with a few layers, while electron energy loss spectroscopy (EELS) confirms their BN composition[11,12]. A disadvantage of this technique is that the yield of BN NTs is not high and contains considerable amounts of nontubular material (e.g. unwanted BN particles, flakes, etc.).

Further developments of the laser technique have continued and, in 1998, the laser ablation of BN powder mixed with nanosized Ni and Co powder in an inert atmosphere (e.g. Ar, N_2, or He) at 1200°C was reported, which resulted in the production of single-, double-, and triple-walled BN NTs[13]. Subsequently, a continuous laser ablation reactor, which employs a rotating catalyst-free BN target under N_2, has been used to generate bulk quantities of samples including single-walled BN NTs[14].

Substitution reactions

In 1998, Han *et al.*[15] reported a novel synthesis method that uses pyrolytically grown CNTs as templates to prepare BN NTs. This technique is able to substitute C atoms with B and N. The authors placed B_2O_3 powder in an open crucible covered by CNTs and maintained the setup under flowing N_2 at 1500°C for 30 min inside an induction furnace (note that thermal furnaces or highly crystalline CNTs do not yield large amounts of BN NTs). After this reaction, BN NTs of similar diameters to the starting CNT material are obtained.

The CNTs, which act as templates, are removed by the intense oxidation conditions caused by B_2O_3, according to the reaction $3C + B_2O_3 \rightarrow 2B + 3CO$. Following this, B and N atoms (supplied during the reaction), may be simultaneously positioned in the vacancies generated within the graphitic network[16], resulting in the formation of BN domains. Interestingly, it has been found that the zigzag chirality dominates the structure of the BN NTs produced using this method (Fig. 3), indicating a high energetic stability[17]. In addition, some of these tubes appear to be open after the substitution reaction. The latter findings are in agreement with *ab initio* molecular dynamics calculations that demonstrate the zigzag BN NTs tend to remain somehow 'open' with amorphous-like material at the tips[18,19].

In 1999, this technique succeeded in producing BN single-walled NTs (SWNTs). Pure C SWNTs were placed with B_2O_3 inside a graphite crucible, which was then heated to 1250°C, 1350°C, and 1530°C over 30 min in a N_2 atmosphere[20]. The authors noted the crucial role of the temperature in the synthesis. It is only possible to obtain pure BN SWNTs at 1350°C as by-products in a sample preferentially composed of B_xC_{1-x} and $B_xC_{1-x-y}N_y$ SWNT bundles; whereas at 1530°C the complete transformation of the C SWNT bundles into bulk BN phases occurs.

It is important to note that the C substitution method is very sensitive to experimental conditions, and it is extremely difficult to remove all C atoms from the generated BN NTs. In this context, Golberg *et al.*[21] claim that the presence of MoO_3 reduces the amount of C remaining as an impurity by adding an extra oxidizing agent to remove the C atoms. Recently, oxidation studies of $B_xC_yN_z$ NTs have been performed using thermogravimetric analysis (TGA)[22]. A brief description of these results can be summarized in four main stages
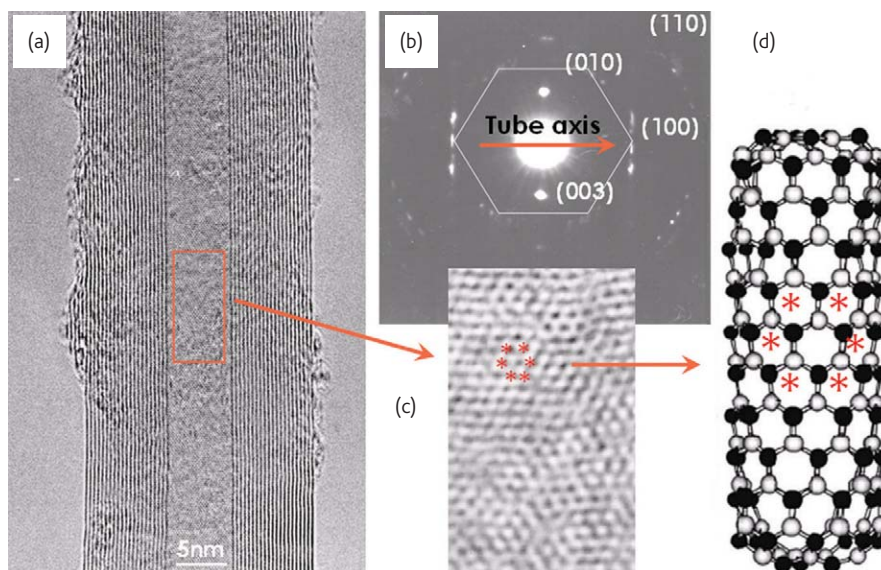

Fig. 3 (a) Representative HRTEM image of a BN NT; (b) electron diffraction pattern of the tube revealing a zigzag chirality; (c) close-up of the image shown in (a) showing the hexagonal array of spots (see red stars for clarity); and (d) molecular model of a zigzag tube with the red spots representing the tube chirality experimentally observed in (a) and (b). (Reprinted with permission from[27]. © 2004 The Royal Society.)

during oxidation: (i) $T_{room} \rightarrow 550°C$: the NTs remain stable; (ii) $550°C \rightarrow 675°C$: the excess of C is removed; (iii) $675°C \rightarrow 800°C$: the mass stabilizes because the C atoms have been oxidized; and (iv) $800°C \rightarrow 1000°C$ BN layers oxidize into B_2O_3 powder. Therefore, the best conditions under which to obtain pure BN NTs from $B_xC_yN_z$ NTs is in air at 700°C for 30 min[22].

Chemical vapor deposition

Five years after the first reports of the synthesis of BN NTs, it became possible to synthesize BN NTs using chemical vapor deposition (CVD). Lourie et al.[23] succeeded using an in situ synthesized precursor (borazin, $B_3N_3H_6$) with NiB or Ni_2B powder as catalyst. The reaction is carried out at 1000-1100°C for 30 min. Other results have been obtained by in situ synthesis of a different precursor, $B_4N_3O_2H$ (Fig. 2b)[24]. In this case, the yield of highly pure BN NTs reached hundreds of milligrams in a single experimental run when B_2O_3 was used as a reactant[25]. Recently, the possibility of producing B-C-N SWNTs using CVD[26] has been shown, although the production of pure BN SWNTs still remains a challenge. The authors obtained B-C-N SWNTs over a powdery MgO-supported Fe-Mo bimetallic catalyst using CH_4, B_2H_6, and ethylenediamine as the reactants in a hot filament (HF) CVD device[26]. It is clear that the CVD technique could be exploited to produce massive quantities of BN NTs, which could be then used for various applications (see below). A complete review of CVD production of BN NTs can be found elsewhere[27].

Ball milling

In 1999, Chen et al.[28] reported an alternative way of producing BN NTs involving the ball milling of elemental B in NH_3 gas followed by thermal annealing at 1000-1200°C under N_2 or Ar. The samples contain bamboo-like NTs composed of BN layers and have diameters of ~50-75 nm. The authors used high-energy ball milling for 150 hours to produce significant structural changes and chemical reactions in the B powder. After the heat treatment, the BN phase can be identified. The presence of Fe (from the milling balls) appears to act as the catalyst. Soon after, Chen and collaborators[29] reported that it is also possible to obtain BN NTs after ball milling h-BN powder for 10 hours following a thermal annealing process. The authors hypothesize that the BN NTs are formed via a solid-state process that involves deposition from vapor, but in which chemical reactions do not occur. The BN NTs also exhibit bamboo-like morphologies and have diameters ranging from 11-280 nm. Subsequently, Chadderton and Chen[30] have proposed that the thermally activated process of surface self-diffusion in the milled powders is the key factor for growing BN NTs and other nanomaterials. The same authors propose a metal tip nanotube growth model. They believe that an Fe particle always located at the tip of the growing tube is responsible for the BN nucleation by a catalytic capillary process. This results in the epitaxial growth of the tube involving preferential planes of Fe and the BN (002) plane[31]. However,

the difference between the diameters of the nanotube ends cannot be explained by this growth scenario.

Recently, Velázquez-Salazar et al.[32] have reported the synthesis and state-of-the-art characterization of BN bamboo-like NTs. The authors demonstrated that:

- The ball milling time induces considerable damage to the h-BN powder after 60 hours, which is less than that used by Chen and collaborators;
- BN NTs always contain a metallic nanoparticle at one end, whereas the other end is closed and does not include a particle of any type;
- A metallic particle (e.g. Fe) appears to be responsible for BN agglomeration and subsequent NT growth;
- No epitaxial relationship is observed between the crystallographic planes of the Fe nanoparticle and the BN (002) plane; and
- The catalytic nanoparticle is not monocrystalline but an agglomeration of various Fe nanocrystals that somehow control the diameter of the BN bamboo-type NTs during growth.

All of these results reveal that the most likely growth mechanism accounting for the formation of bamboo-like BN NTs is the root-growth process catalyzed by Fe nanoparticles. Fig. 4 depicts scanning electron microscopy (SEM) images and the mechanism proposed by Velázquez-Salazar and collaborators.

Very recently, Fengqiu et al.[33] have claimed that it is possible to grow BN NTs by annealing a ball-milled B powder in NH_3 without involving a catalytic nanoparticle. However, further studies are required to improve the yields of BN NTs using this technique.

Alternative experimental approaches have also been developed in order to generate BN NTs and other BN nanostructures: (i) thermal annealing of powdered β-rhombohedral B and h-BN mixtures at 1200°C in Li vapor[34]; (ii) plasma jets[35]; (iii) plasma-assisted laser vapor deposition[36]; (iv) pyrolysis of melamine diborate ($C_3H_6N_6.2H_3BO_3$) in the absence of a metal catalyst[37], etc. It is noteworthy that in the latter method, BNO clusters are responsible for the growth of BN NTs.

BN NT chemistry and purification

Last year, the first reports describing the purification of BN NTs appeared[38,39]. Chen et al.[38] reported a four step purification process: (i) dispersion of large aggregates by ultrasonic treatment in ethanol; (ii) removal of metal particles by selective chemical leaching with HCl; (iii) dissolution of BN particles by selective oxidation at 800°C in air; and (iv) hot water washing and filtering to remove the B_2O_3 residues.

The second work[39] focused on the removal of BN impurities (e.g. nanoparticles, ribbons, and amorphous material) from NTs using the strong interactions between BN NTs and a conjugated polymer. The conjugated polymer selectively wraps around (covers) BN NTs and can then be used to differentiate between BN NTs and BN impurities. In this case, a three-step purification process is used: (i) the sample is washed by HNO_3 to remove catalytic particles; (ii) a conjugated polymer, poly(m-phenylenevinylene)-co-(2,5-dioctoxy-p-phenylene) or
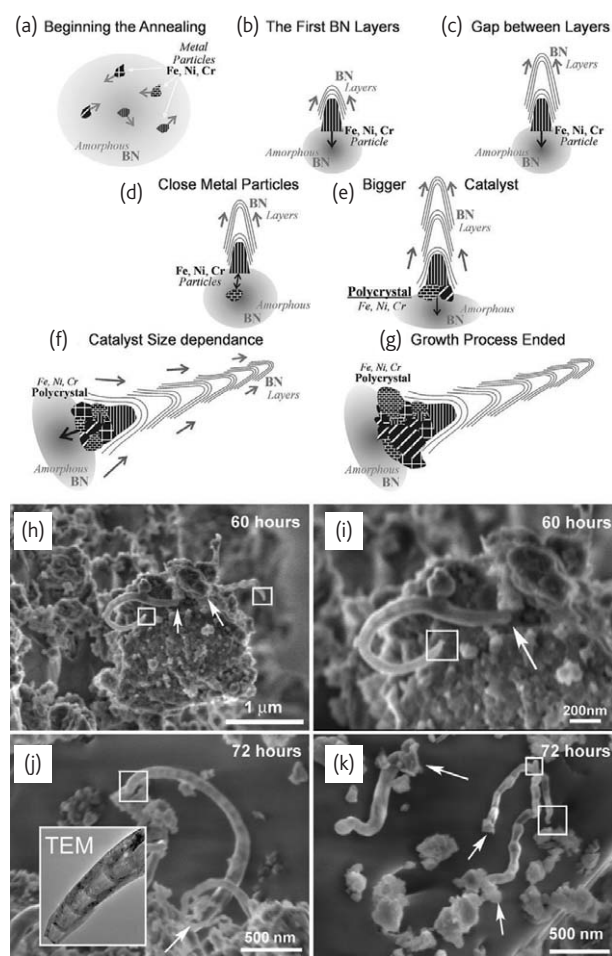
Fig. 4 Schematic diagram of BN NT growth during the annealing part of the ball-milling process: (a) small Fe-based alloy nanoparticles are spread in the BN amorphous material after ball milling; (b) as the temperature is increased, BN material starts to migrate and precipitate layers, which adopt the shape of small Fe-based alloy nanoparticles; (c) sliding of the first cone-shaped cup-like structure occurs as a result of the strains created inside the cup, leaving a gap below the tip; (d) repetition of the process resulting in agglomeration of additional Fe-based alloy nanoparticles, which start to attach to other metal particles; (e) following the coalescence of various metallic particles, the seeding particle increases in size, resulting in an enlargement of the precipitated BN cups; (f) the metal agglomeration process continues, as well as the sliding of the cups, resulting in NT growth; (g) Fe-based particles reach a critical size that inhibits the formation of additional BN layers and the growth process is interrupted. Scanning electron microscope (SEM) images showing BN NTs produced after annealing amorphous BN powders obtained from h-BN powders ball milled for 60 hours (h-i) and 72 hours (j-k). Note that these fibers are always attached to a larger particle (indicated by white arrows). A TEM image of a typical BN NT end is also shown in the inset of (j). Squares denote the thin end of the tubular BN structure. (Reprinted with permission from[32]. © 2005 Elsevier.)

PmPV, is used to wrap the BN NTs by mixing the PmPV and BN NTs in chloroform, which makes the wrapped BN NTs soluble, after which the mixture is centrifuged, accompanied by the removal of insoluble material (BN impurities); and (iii) heat treatment of the composite

material in air at 700°C removes the PmPV wrapping and extracts the BN NTs (see below).

Mechanical and electronic properties

The mechanical properties of C, BN, BC_3, and BC_2N NTs have been studied theoretically by Hernández et al.[40] using a nonorthogonal tight-binding model. The authors found that BN NTs have a lower (by about 30%) Young's modulus compared with CNTs, although it is still of the same order of magnitude. Experimental determination of the Young's modulus of multiwalled BN NTs has also been carried out ($Y = 1.22 \pm 0.24$ TPa)[41], confirming the values obtained by theoretical approaches. The results indicate that BN NTs are highly crystalline and may be the most robust insulating nanofiber ever synthesized.

It is interesting to note that axial compression of BN NTs has also been studied using tight-binding molecular dynamics[42]. The authors found that for the same (8,0) zigzag NTs, the C specimen has a lower calculated elastic limit than its BN counterpart. This can be explained by both a lower Young's modulus and the buckling in the structure that results from rotated BN bonds. The accumulated strain is accommodated by increasing the rotation angle of the BN bonds that are parallel to the tube axis before it undergoes a transition causing a plastic deformation. The lack of bonds parallel to the tube axis in armchair BN NTs explains why they do not reveal such an effect.

Mechanical deformation of BN NTs affects their electronic properties because of changes in the hybridization of orbitals. Kim et al.[43] have proposed that high pressures collapse BN NTs. Their calculations using *ab initio* approaches with the LDA demonstrate that, for a (9,0) zigzag BN NT, the compression causes a reduction in the bandgap from 3.5 eV to 1.0 eV as the tube is flattened from 0.74 nm to 0.20 nm. The authors estimate that 10 GPa is enough to collapse BN NTs with diameters of 3 nm, and could result in bandgaps of about 2 eV. The authors also found that the energy gap of armchair NTs is less sensitive to pressure, reducing by only about 0.6 eV when they are flattened below the van der Waals interaction distance.

From the experimental standpoint, a comparative high-pressure Raman study of BN NTs up to 16 GPa and h-BN up to 21 GPa has been carried out at room temperature in a diamond anvil cell[44]. The BN NTs are observed to undergo an irreversible phase transition at a pressure of ~12 GPa, which is different from the values reported for CNTs (~20 GPa)[45].

When BN NTs are subjected to a high dc electric field, the electronic density of states is modified. Khoo et al.[46] have performed *ab initio* calculations within the generalized gradient approximation (GGA) of the effects of a transverse electric field on the energy gap of BN NTs. The results show that the energy gap decreases linearly with increasing electric field. They also show that, for a given field strength, the energy gap reduction is greater for large diameter NTs and the effect is independent of chirality. Meunier et al.[47] have found that the polarization of an electric field can be used to lower the work function

of BN/C NT tips, thereby increasing the field-emitting properties over CNT tips by up to two orders of magnitude.

Defects in BN NTs

As mentioned above, the caps of BN NTs are different from pure CNTs; the presence of pentagons in BN NT caps is not energetically favored. In general, capped BN NTs usually exhibit sharp caps and it has been proposed that either three squares (B_2N_2)[7,8], combinations of four squares (B_2N_2) and one octagon (B_4N_4)[8], or three pairs of pentalene units containing an excess of N atoms[48] could be responsible for the tube closure. However, it still has not been confirmed which type of BN defect appears within BN NT caps. Therefore, additional research should continue in this direction.

Blase et al.[18] have calculated theoretically that pentagon-heptagon defects are unstable in BN NTs since they produce a bond frustration effect. This effect implies the presence of two atoms of the same type next to each other (a B-B or a N-N bond), which has a higher energy cost. Using ab initio molecular dynamics, the authors found that armchair edges tend to close dangling bonds, creating square defects and closing the NTs, whereas zigzag edges possess dangling bonds that close and reopen during the simulation.

Very recently, the formation of defects in BN NTs by electron irradiation with an electron microscope has been reported by Zobelli et al.[49]. The authors demonstrate that divacancies are created under electron irradiation. Theoretical results indicate that, by clustering these divacancies, the system becomes energetically stable. This results in chirality changes or significant deformations within tubes. Interestingly, these defective tubes do not significantly change the electronic bandgap but introduce acceptor states into it. Therefore, it is expected that defective tubes will still behave as insulators. Further discussion regarding defects in NTs can be found elsewhere[49].

Doped BN NTs, hetero-NTs, and magnetic properties

As discussed above, BN NTs are mainly insulators. However, it is also possible to reduce the electronic bandgap by adding C atoms into the structure. For example, the substitution reaction synthesis method could well yield C-doped BN NTs.

In this context, theoretical calculations have been performed and it has been demonstrated that the electronic bandgap is reduced as additional C atoms are introduced into the hexagonal BN network[50,51] (Fig. 5). As more C is introduced into the h-BN network, Mazzoni et al.[51] demonstrate theoretically that the $B_3C_2N_3$ stoichiometry is more stable than BC_2N, which had been predicted previously to be more stable[52]. However, from the experimental standpoint, Watanabe and coworkers[53,54] have found that layered BC_2N compounds (not NTs) are able to emit light in the visible range. Therefore, experimental determination of the bandgap, using scanning tunneling microscopy (STM), and the electronic transport in C-doped BN NTs should be

carried out in the near future to determine the most stable phases of these novel layered and tubular systems.

The idea of BN/C heterostructured NTs was initially explored by Blase and coworkers[55] using density functional theory (DFT) within the LDA and semi-empirical approaches[50]. They estimate the formation energy of the C/BN interfaces to be ~0.4 eV per interface bond. They have also studied the interdiffusion process in a C/BN interface, and find that this process would have an energy cost close to 2.0 eV per atom, making it very unlikely and favoring abrupt interfaces.

BCN heterostructured NTs can also exhibit physico-chemical properties that are intermediate between those of their pure counterparts. A heterojunction between a metallic CNT and a BN NT has different properties depending on the relative composition of the structure. In Fig. 5, different heterojunctions corresponding to a (5,5) NT from $(BN)C_4$ to a pure BN NT are depicted. The densities of states were calculated using the LDA to DFT and norm-conserving pseudopotentials implemented using the SIESTA code[56]. As the BN content is increased, the energy gap increases from 0.15 eV to 4.2 eV. These results are consistent with previous reports on supercell
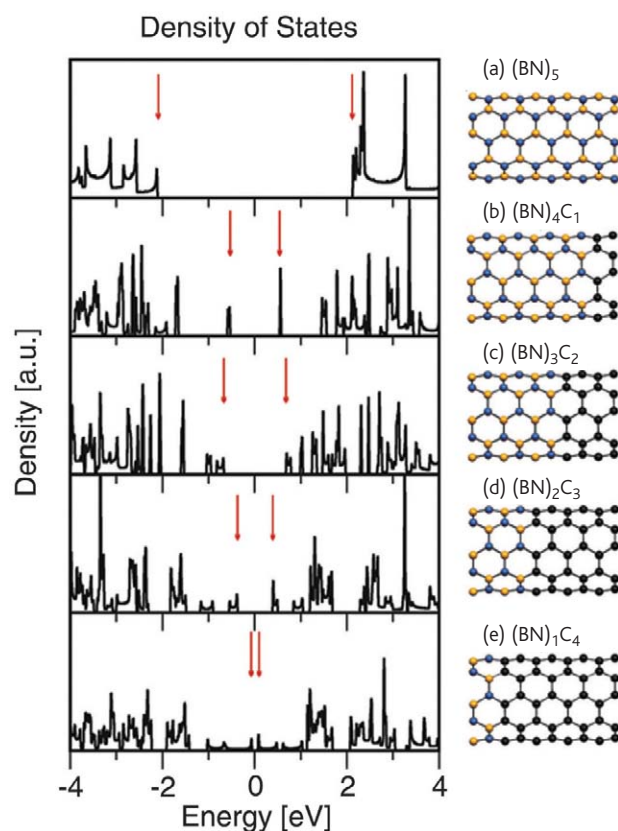

Fig. 5 Densities of states for BN/C NT heterojunctions with different stoichiometries, from pure BN to $(BN)C_4$. The top valence and bottom conduction states are indicated with red arrows. The energy gap in these NTs varies from 0.15-4.2 eV as the BN content is increased, with the exception of $(BN)_4C_1$, where two defect-like nondispersive energy states reduce the energy gap.

geometries for C/BN NT heterojunctions[57]. In a recent work, Guo *et al.*[58] describe the synthesis of C/BN multiwalled NT heterojunctions using a two-stage hot filament CVD (HFCVD) process with varying flows of the C, B, and N sources under a polycrystalline Ni substrate. This suggests that this kind of heterostructures could be synthesized in a controlled way in the near future.

Besides the effect of C on BN NT properties, it is also possible to produce Si-doped BN NTs via catalyst-assisted pyrolysis of a B- and Si-containing polymeric precursor[59]. The precursor is mixed with $FeCl_2$ powder and subjected to high-energy ball milling for 70 hours. The mixture is then heat treated at 1350°C for 3 hours under a N_2 atmosphere; the resulting Si content in the BN tubes is ~6 wt.%. Therefore, the concept of doping BN NTs with different elements needs to be followed up from the theoretical and experimental standpoints.

Analogous to the edge states present in nanosized graphite, there are edge states in h-BN and open BN NTs. These edges, along with heterostructured BCN nanosized ribbons, have been studied by Okada and Oshiyama[60]. The authors found that particular BNC ribbon geometries are ferromagnetic. In later work, Nakamura *et al.*[61] found that other BN-decorated graphite ribbons have a ferrimagnetic ground state caused by unbalanced occupation of the border and edge states.

A theoretical study of the electronic and magnetic properties of C and BN heterostructured NTs has been carried out by Choi and coworkers[57,62]. The authors studied several decorations of the hexagonal lattice and found that there is a spin polarization present in the border states of a zigzag (9,0) NT decorated with alternate zigzag rings of C and BN when doped with two holes. It is clear that magnetic and electronic BN ribbons and hetero-NTs (e.g. BCN, C-doped BN, etc.) should exhibit unsusual magnetic and electronic properties and are, therefore, worth investigating further.

Other BN nanomaterials

Besides BN NTs, other nanostructures have been successfully synthesized using different techniques. Huo *et al.*[63] have reported the preparation of BN nanowires (NWs) via the reaction of a mixture of NH_3 and N_2 gas flowing over α-FeB nanoparticles at 1100°C. HRTEM images reveal perfectly straight lattice fringes with interlayer spacings of ~3.33 Å. It is also likely that, besides these NWs, BN ribbons could form, but additional characterization of these materials is required. Other studies have demonstrated the presence of different nanostructures composed of B, C, and/or N, including BN NWs[64].

BN NWs exhibiting stacked cone morphologies have been obtained in high yields using the ball milling thermal method and pure B_4C powder. The milled powders are placed on a Si wafer that has a layer of ferric nitrate ($Fe(NO_3)_3$) and heated to 450°C for ~1 hour to activate the catalyst particles. The temperature is then increased to 1300°C and kept at this level for over 8 hours. All heat treatments are performed under a N_2 atmosphere. A metallic alloy of Fe-Si is observed at the tips of each BN NW[65]. Recently, pure BN NWs containing turbostratic
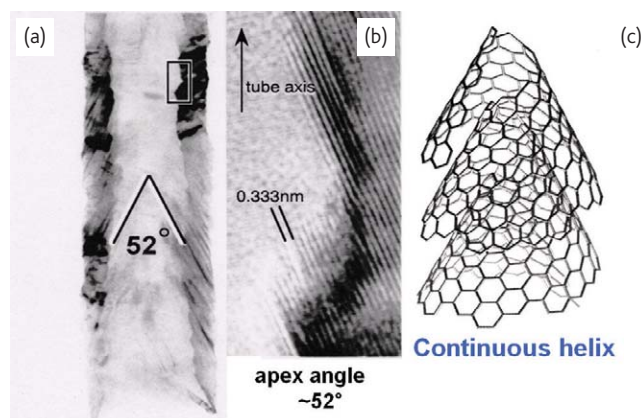

Fig. 6 (a) TEM images of a helically folded conical tube showing a hollow core; (b) HRTEM image of the tubes revealing an apex angle of 52° and interlayer spacings of 0.33 nm; and (c) molecular model explaining the structures shown in (a) and (b). (Courtesy of F. F. Xu. Reprinted with permission from[68]. © 2003 American Chemical Society.)

BN layers have been produced with high yields without any catalyst particle on the tips by heating BI_3 powder under an NH_3 atmosphere at 1100°C[66]. The same group has also reported the growth of h-BN NWs by heating B and ZnO powders at 1100°C under a N_2:H_2 flow using stainless-steel foils as substrate and catalyst[67].

Besides different types of NWs, other BN nanomorphologies have been synthesized. For example, BN helical conical NTs (Fig. 6), which correspond to hollow cylindrical structures but where the walls are not parallel to the tube axis. Apex angle measurements and diffraction patterns indicate that these structures consist of a BN ribbon wrapped in a helicoidal fashion[68].

In addition, BN nanocones can be synthesized using a substitution reaction process with CNTs as templates[69]. Arc-melting methods have also been used to synthesize multiwalled BN nanohorns[70]. The field-emission properties of BN cones under an electric field have been studied theoretically and indicate that, depending on the geometry of the tip, these structures could be used as probes in electronic microscopy and as efficient field emitters[71,72]. Moreover, negative Gaussian curvature introduced by the presence of octagonal rings with alternating B and N atoms is possible in BN structures[48]. Saddle shape defects could therefore be used to modify the electronic behavior of BN nanocones[73]. Certainly, the introduction of defects and doping at the tips of BN nanocones plays an important role in the electronic and emission properties of these fascinating nanoarchitectures[74] and constitutes an interesting field for experimentalists.

Perspectives and conclusions

We have shown that BN nanotube research has developed rapidly over the past three years. The first synthetic method was reported 12 years ago and we have since then witnessed the production of novel BN nanostructures. Although some chemistry-oriented work involving BN NTs has just been reported, we envisage more new chemistry arising

from these tubes (Fig. 7). In this context, we expect work related to the functionalization and solubilization of BN SWNTs, the attachment of metal nanoparticles (Ag, Au, Pt, etc.) on BN NTs, etc., to be realized in the future.

It is clear that pure BN NTs will always behave as insulators. However, we have shown that doping with defects, C, or Si could be possible and that these doped tubes are expected to behave as narrow bandgap semiconductors. By controlling the level of doping it should also be possible to tune the bandgap of BN NTs. Therefore, additional experimental and theoretical work related to the doping of BN NTs will be of paramount importance within the next years.

An exciting issue that needs further experimental study is related to the magnetism and optical properties of doped BN NTs. We believe that novel properties will be discovered. Very recently, for example, Arenal et al.[75] used EELS to determine the optical gap and found values of ~5.8 ± 0.2 eV for different tubes (single-, double-, and triple-walled). In addition, Watanabe and colleagues[76] have demonstrated experimentally that pure h-BN (not NTs) could be used in lasers emitting in the ultraviolet region at room temperature.

Although significant advances in the synthesis of multiwalled BN NTs have been made, further research is needed to produce BN SWNTs. The physics of these tubes could be quite exciting, but purer samples are required. In this context, novel assembly approaches for obtaining C-BN-C two- and three-dimensional covalent hetero-networks need to be developed (Fig. 8). It is expected that such arrays could represent a step toward nanoelectronics where the generated network ('nano-circuit') could present different electronic paths through a BN NT or a CNT[77].

Very recently, it has been shown that mesoporous BN materials can be generated using substitution reactions involving mesoporous C as templates[78,79]. Therefore, the H_2 adsorption and catalytic properties of mesoporous BN need to be explored. In addition, the controlled synthesis of BN ribbons requires further experimental and theoretical work.

Besides NTs, NWs, ribbons, and mesoporous BN, other BN nanostructures exhibiting novel physico-chemical properties are likely to be reported in the future. We also expect that applications of BN NTs and nanostructures will appear shortly. We envisage that doped BN NTs could be used as stable field emitters with low turn-on voltages or efficient gas sensors. In addition, insulating and robust polymer composites using BN NTs are likely to appear (Fig. 7). These composites are expected to be superior to bulk BN-composites[80]. However, methods capable of producing large quantities of these nanostructures, at reasonable costs, need to be developed.

Other optical and magnetic applications using BN NTs will also arise, however the presence of defects and impurities may be the key issue to control and tune the properties. In this context, novel photogalvanic effects that have been predicted theoretically[81,82] could be found experimentally in ceramic NTs. Very recently, Bai
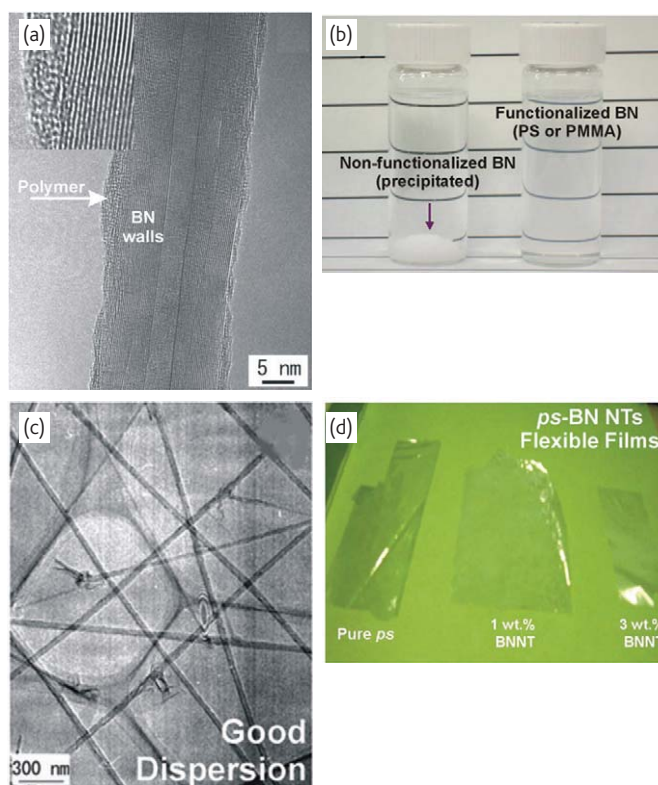

Fig. 7 (a) HRTEM image of a BN NT coated with PmPV (inset shows the amorphous-like material, i.e. the polymer, coating the NT surface); (b) images of two vials containing BN NT (in a solvent – chloroform), note that the vial on the left shows BN NT precipitation at the bottom of the vial because the tubes were not functionalized with a polymer and are not soluble, whereas the vial on the right does not reveal precipitation because of preliminary BN NT functionalization with polystyrene (PS) or poly(methyl methacrylate) (PMMA); (c) TEM image of a BN NT solution displaying pure BN NTs; and (d) composite films of PS with BN NTs after adding 1 wt.% or 3 wt.% multiwalled BN NTs, note that the films are still transparent. (Courtesy of C. Y. Zhi.)
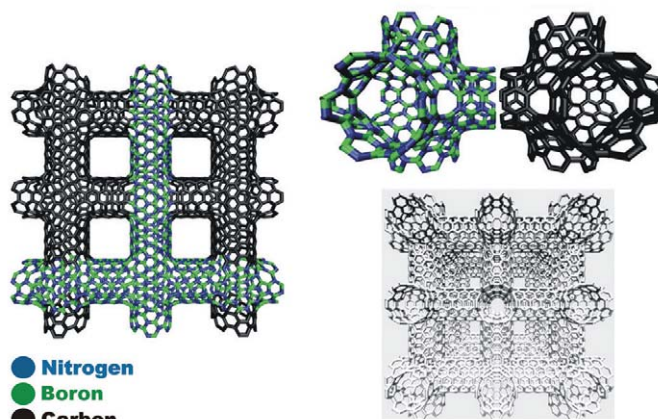

Fig. 8 Molecular models of two- and three-dimensional BN-C networks showing the possibility of constructing heteronetworks that could exhibit unusual and novel electronic and mechanical properties.

and coworkers[83] have found that BN NTs, which are insulating, may become semiconducting by bending the tubular structure.

Keeping in mind hollow BN channels, some recent results have demonstrated the encapsulation of various materials including halides[84], SiC[85], Fe[86], B_4C[87], Al_2O_3[24], ferromagnetic alloys[88], and others. In the near future, the properties of these filled BN NTs will be studied in detail.

In summary, we have briefly reviewed the most significant achievements related to the production, properties, and applications of BN and doped BN NTs. We believe that in the following years this field will develop quickly and it is possible that, for certain applications, BN NTs could replace pure CNTs. However, focused research is necessary. mt

REFERENCES

1. Blase, X., *et al.*, *Phys. Rev. B* (1995) **51**, 6868
2. Rubio, A., *et al.*, *Phys. Rev. B* (1994) **49**, 5081
3. Hamada, N., *et al.*, *Phys. Rev. Lett.* (1992) **68**, 1579
4. Mintmire, J. W., *et al.*, *Phys. Rev. Lett.* (1992) **68**, 631
5. Blase, X., *et al.*, *Europhys. Lett.* (1994) **28**, 335
6. Chopra, N. G., *et al.*, *Science* (1995) **269**, 966
7. Loiseau, A., *et al.*, *Phys. Rev. Lett.* (1996) **76**, 4737
8. Terrones, M., *et al.*, *Chem. Phys. Lett.* (1996) **259**, 568
9. Terrones, M., *et al.*, *Carbon* (2002) **40**, 1665
10. Cumings, J., and Zettl, A., *Chem. Phys. Lett.* (2000) **316**, 211
11. Golberg, D., *et al.*, *Appl. Phys. Lett.* (1996) **69**, 2045
12. Golberg, D., *et al.*, *Chem. Phys. Lett.* (1997) **279**, 191
13. Yu, D. P., *et al.*, *Appl. Phys. Lett.* (1998) **72**, 1966
14. Lee, R. S., *et al.*, *Phys. Rev. B* (2001) **64**, 121405
15. Han, W., *et al.*, *Appl. Phys. Lett.* (1998) **73**, 3085
16. Golberg, D., *et al.*, *Solid State Commun.* (2000) **116**, 1
17. Golberg, D., *et al.*, *Appl. Phys. Lett.* (2000) **77**, 1979
18. Blase, X., *et al.*, *Phys. Rev. Lett.* (1998) **80**, 1666
19. Charlier, J.-C., *et al.*, *Appl. Phys. A* (1999) **68**, 267
20. Golberg, D., *et al.*, *Chem. Phys. Lett.* (1999) **308**, 337
21. Golberg, D., *et al.*, *Chem. Phys. Lett.* (2000) **323**, 185
22. Han, W.-Q., *et al.*, *Appl. Phys. Lett.* (2002) **81**, 1110
23. Lourie, O. R., *et al.*, *Chem. Mater.* (2000) **12**, 1808
24. Ma, R., *et al.*, *Chem. Mater.* (2001) **13**, 2965
25. Zhi, C., *et al.*, *Solid State Commun.* (2005) **135**, 67
26. Wang, W. L., *et al.*, *J. Am. Chem. Soc.* (2006) **128**, 6530
27. Ma, R., *et al.*, *Philos. Trans. R. Soc. London, Ser. A* (2004) **362**, 2161
28. Chen, Y., *et al.*, *Chem. Phys. Lett.* (1999) **299**, 260
29. Chen, Y., *et al.*, *Appl. Phys. Lett.* (1999) **74**, 2960
30. Chadderton, L. T., and Chen, Y., *Phys. Lett. A* (1999) **263**, 401
31. Chadderton, L. T., and Chen, Y., *J. Cryst. Growth* (2002) **240**, 164
32. Velázquez-Salazar, J. J., *et al.*, *Chem. Phys. Lett.* (2005) **416**, 342
33. Fengqiu, J. I., *et al.*, *J. Chem. Eng.* (2006) **14**, 389
34. Terauchi, M., *et al.*, *Chem. Phys. Lett.* (2000) **324**, 359
35. Shimizu, Y., *et al.*, *Appl. Phys. Lett.* (1999) **75**, 929
36. Komatsu, S., *et al.*, *J. Appl. Phys.* (2002) **91**, 6181
37. Ma, R., *et al.*, *Chem. Phys. Lett.* (2001) **337**, 61
38. Chen, H., *et al.*, *Chem. Phys. Lett.* (2006) **425**, 315
39. Zhi, C., *et al.*, *J. Phys. Chem. B* (2006) **110**, 1525
40. Hernández, E., *et al.*, *Phys. Rev. Lett.* (1998) **80**, 4502
41. Chopra, N. G., and Zettl, A., *Solid State Commun.* (1998) **105**, 297
42. Srivastava, D., *et al.*, *Phys. Rev. B* (2001) **63**, 195413
43. Kim, Y.-H., *et al.*, *Phys. Rev. B* (2001) **63**, 205408
44. Saha, S., *et al.*, *Chem. Phys. Lett.* (2006) **421**, 86
45. Karmakar, S., *et al.*, *Phys. Rev. B* (2001) **69**, 165414
46. Khoo, K. H., *et al.*, *Phys. Rev. B* (2004) **69**, 201401
47. Meunier, V., *et al.*, *Appl. Phys. Lett.* (2002) **81**, 46
48. Fowler, P. W., *et al.*, *Chem. Phys. Lett.* (1999) **299**, 359
49. Zobelli, A., *et al.*, *Nano Lett.* (2006) **6**, 1955
50. Blase, X., *et al.*, *Appl. Phys. A* (1999) **68**, 293
51. Mazzoni, M. S. C., *et al.*, *Phys. Rev. B* (2006) **73**, 073108
52. Miyamoto, Y., *et al.*, *Phys. Rev. B* (1994) **50**, 4976
53. Watanabe, M. O., *et al.*, *Phys. Rev. Lett.* (1996) **77**, 187
54. Chen, Y., *et al.*, *Phys. Rev. Lett.* (1999) **83**, 2406
55. Blase, X., *et al.*, *Appl. Phys. Lett.* (1997) **70**, 197
56. Soler, J. M., *et al.*, *J. Phys. Cond. Matter* (2002) **14**, 2745
57. Choi, J., *et al.*, *Phys. Rev. B* (2003) **67**, 125421
58. Guo, J. D., *et al.*, *Appl. Phys. Lett.* (2002) **80**, 124
59. Fan, Y., *et al.*, *J. Am. Ceram. Soc.* (2006) **89**, 740
60. Okada, S., and Oshiyama, A., *Phys. Rev. Lett.* (2001) **87**, 146803
61. Nakamura, J., *et al.*, *Phys. Rev. B* (2005) **72**, 205429
62. Kim, Y.-H., *et al.* *Phys. Rev. B* (2003) **68**, 125420
63. Huo, K. F., *et al.*, *Appl. Phys. Lett.* (2002) **80**, 3611
64. Deepak, F. L., *et al.*, *Chem. Phys. Lett.* (2002) **353**, 345
65. Zhang, H., *et al.*, *J. Am. Ceram. Soc.* (2006) **89**, 675
66. Chen, Y. J., *et al.*, *Nanotechnology* (2006) **17**, 786
67. Chen, Y. J., *et al.*, *Nanotechnology* (2006) **17**, 2942
68. Xu, F.-F., *et al.*, *J. Am. Chem. Soc.* (2003) **125**, 8032
69. Bourgeois, L., *et al.*, *Phys. Rev. B* (2000) **61**, 7686
70. Nishiwaki, A., and Oku, T., *J. Electron Micros.* (2005) **54**, I9
71. Machado, M., *et al.*, *Chem. Phys. Lett.* (2004) **392**, 428
72. Azevedo, S., and de Brito Mota, F., *Int. J. Quantum Chem.* (2006) **106**, 1907
73. Azevedo, S., *J. Solid State Chem.* (2005) **178**, 3090
74. An, W., *et al.*, *J. Phys. Chem. B* (2006) **110**, 16346
75. Arenal, R., *et al.*, *Phys. Rev. Lett.* (2005) **95**, 127601
76. Watanabe, K., *et al.*, *Nat. Mater.* (2004) **3**, 404
77. Romo-Herrera, J. M., *et al.*, *Nano Lett.* (2007) **7**, 570
78. Vinu, A., *et al.* *Chem. Mater.* (2005) **17**, 5887
79. Han, W.-Q., *et al.*, *Nano Lett.* (2004) **4**, 173
80. Kim, D.-P., *et al.*, *J. Am. Ceram. Soc.* (1995) **78**, 1546
81. Mele, E. J., and Král, P., *Phys. Rev. Lett.* (2002) **88**, 056803
82. Král, P., *et al.*, *Phys. Rev. Lett.* (2000) **85**, 1512
83. Bai, X., *et al.*, *Nano Lett.* (2007) **7**, 632
84. Han, W.-Q., *et al.*, *Nano Lett.* (2004) **4**, 1355
85. Han, W. Q., *et al.*, *Appl. Phys. Lett.* (1999) **75**, 1875
86. Ma, R., *et al.*, *Chem. Phys. Lett.* (2001) **350**, 1
87. Ma, R., *et al.*, *Chem. Phys. Lett.* (2001) **350**, 434
88. Bando, Y., *et al.*, *Chem. Phys. Lett.* (2001) **347**, 349